Table 1 Apollo landing site solutions

Apollo mission		Latitude, degs[a]	Latitude solution sigma, degs	Longitude, degs	Longitude solution sigma, degs
Apollo 11	Star/g	0.612	0.020	23.498	0.014
	Best	0.647	0.020	23.505	0.006
Apollo 12	Star/g	−3.045	0.025	−23.423	0.018
	Best	−3.043	0.014	−23.416	0.004
Apollo 14	Star/g	−3.652	0.021	−17.466	0.018
	Best	−3.650	0.014	−17.478	0.004

[a] 0.001° is approximately 100 ft on lunar surface.

ϕ and λ. The effect of the erroneous potential model is evident in the characteristics of the convergence and in the final solution. The error in the final solution is 0.463° in ϕ and 4.662° in λ, which agrees within 5% with that obtained using Eq. (8).

The filter defined herein has been used on the Apollo program for missions 11, 12, and 14 to determine the landing coordinates of the Lunar Module. The solutions obtained from the star-gravity filter and the solutions currently considered to be the best landing site estimates are given in Table 1.

The noise used for processing these mission data was 1.0 mrad and is reflected in the solution standard deviation. However, the solution accuracy does not include gravity model uncertainties (the L1 potential model was used for processing these mission data). The best solutions given for comparison were those obtained from all solution sources, including the following: a) Command Module optical tracking of Lunar Module, b) Lunar Module radar tracking of Command Module, and c) Lunar mapping verified by visual sightings.

The solution accuracy given for the best solution was estimated from the manned spaceflight tracking accuracy, the accuracy of the Command Module sextant and the Lunar Module radar, and the accuracy of lunar maps. The comparison of these results indicate that the performance of the filter is reasonably close to the predicted performance.

Conclusions

A filter has been developed to determine position on a planet surface from measurements of star vectors and gravity vectors in a common coordinate system. An advantage in this formulation is the allowance of a measurement coordinate frame which changes between sets of star-gravity measurements. The accuracy of this filter has been shown to be comparable to other available solutions for the Apollo landing missions and to have a limiting accuracy determined by the uncertainty of the potential model. In summary, this technique appears to provide a viable method for determining position on a planet surface.

Cone Transitional Boundary-Layer Structure at $M_e = 14$

MICHAEL C. FISCHER* AND LEONARD M. WEINSTEIN*
NASA Langley Research Center, Hampton, Va.

Nomenclature

M = Mach number
P = pressure, N/m^2
$\dot{q}$ = convective heat-transfer rate, W/m^2
Re/m = local unit Reynolds number
T = temperature, °K
x = distance along cone surface from tip, m
y = distance perpendicular to cone surface, cm
δ = boundary-layer thickness, $dP_{t,2}/dy = 0$, cm
δ^* = displacement thickness, cm
θ = momentum thickness, cm
ϕ_{spread} = disturbance total spreading angle, deg.
ϕ_{wall} = disturbance spreading angle relative to wall, deg.
α = angle of attack, deg.

Subscripts
2 = behind normal shock
e = boundary-layer edge conditions
survey = survey station
t = total conditions
tr = start of transition
w = wall condition
∞ = freestream condition

Received September 28, 1971.

* Aerospace Engineers, Viscous Flows Section, Hypersonic Vehicles Division.

In classical boundary-layer analysis, three general flow regimes may be distinguished dependent on the stability of the flow[1]; steady laminar flow, nonsteady laminar flow oscillations-transitional flow, and turbulent flow. The second regime, that dealing with the growth of the initial instability into developed turbulent flow, is the least understood and most difficult to model. Results from studies using hot-wire and hot-film instrumentation[2-7] indicate that significant oscillations occur far upstream of the transition location at the surface. At low speeds the large oscillations in the laminar boundary layer apparently do not influence the mean laminar velocity profile or the thickness parameters δ, δ^*, and θ, since good agreement with the laminar Blasius solution has been obtained.[2,3] However, at high speeds, more extreme oscillations occur ahead of the surface transition location[4-7]; consequently, the growth of disturbances at the boundary-layer edge may significantly alter the "laminar" boundary-layer profiles, thicknesses, and integral parameters. Morkovin[8] points out that a significantly altered transition region probably occurs at hypersonic speeds as compared to lower speeds.

This Note proposes to determine if the laminar profiles and thicknesses are altered significantly in the outer half of a hypersonic boundary layer upstream of the nominal wall transition location. The tests were conducted in the Mach 20 leg of the Langley High Reynolds Number Helium facility which has a 1.525-m-diam test section and an axisymmetric contoured

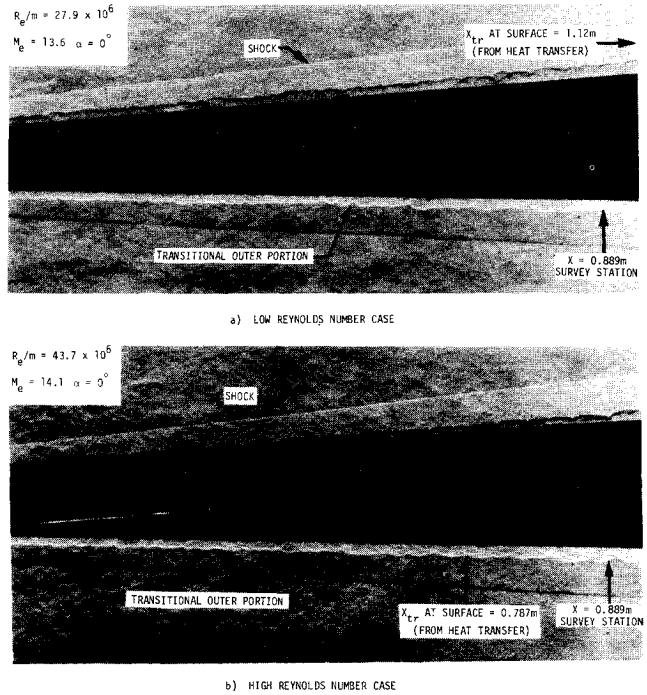

Fig. 1 Spark schlierens of a 2.87° half-angle cone in helium at $M_\infty \approx 18$.

nozzle. Pitot surveys, heat transfer, spark schlierens and wall pressure measurements were obtained at zero angle of attack on a 2.87° half-angle, 1.525 m long smooth cone, with a nose radius of 0.0102 cm. Model instrumentation consisted of pressure orifices and thermocouples for heat transfer determination from which the wall transition location was obtained. Two Pitot surveys were obtained at $x = 0.889$ m; one at $Re/m = 27.9 \times 10^6$ and another at $Re/m = 43.7 \times 10^6$. The Pitot probe diameter was 0.102 cm. The tests were conducted in unheated flow ($T_{t,\infty} = 300°K$) and with $T_w/T_{t,\infty} \simeq 1.0$.

Spark schlierens of the cone for each of the two test Reynolds numbers are shown in Fig. 1. Note the wavy appearance of the boundary-layer edge with protuberances having a scale on the order of twice the boundary-layer thickness. A similar rope-or-chainlike structure at the boundary-layer edge was observed by Potter and Whitfield[9] prior to the surface transition location on a cone at $M_e = 8.0$. For the low Reynolds number case (Fig. 1a) the Pitot survey was obtained upstream of the surface transition location, that is $x_{survey} = 0.794x_{tr}$. For the high Reynolds number case (Fig. 1b) transition at the surface had moved forward such that $x_{survey} = 1.13x_{tr}$.

The Pitot surveys were reduced to Mach number profiles (presented in Fig. 2) using measured values of wall static pressure and assuming constant static pressure across the boundary-layer. Also shown in Fig. 2 are a theoretical laminar similar solution based on the method of Ref. 10 and measured heat-transfer distributions from which the surface transition location was determined. Since these tests were conducted at $T_w/T_{t,\infty} \simeq 1.0$, the heat flux was from the model to the flow ($-\dot{q}$). The decrease in $\dot{q}$ from the laminar $\frac{1}{2}$-power slope, attributed to the variation of the recovery factor through the transition region, marks the start of transition location. The survey obtained upstream of the surface transition location ($x_{survey} = 0.794x_{tr}$) indicated that the outer part of the boundary-layer was transitional as expected from the spark schlieren (Fig. 1a). The experimental boundary-layer thickness for this case was 1.02 cm, about 15% greater than the laminar similar solution prediction. The Mach number profile obtained at the high Reynolds number case ($x_{survey} = 1.13x_{tr}$) indicated a well developed transition process at the survey station, even though transition at the wall had just occurred a short distance upstream.

The results of the present study suggest that in hypersonic

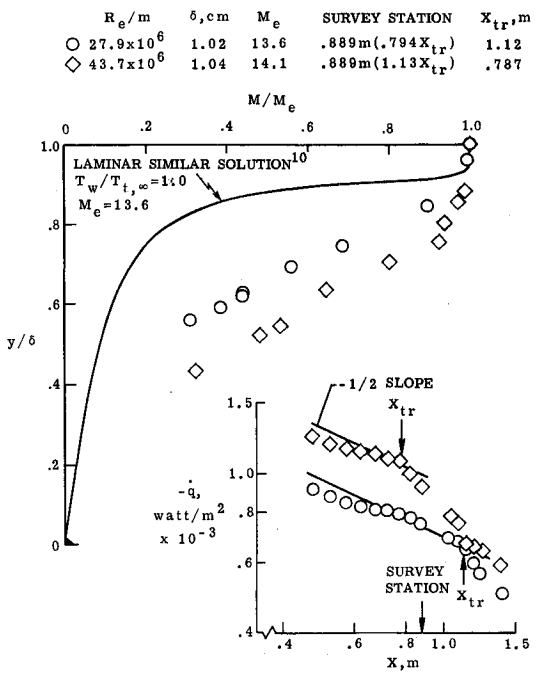

Fig. 2 Experimentally determined Mach number profiles and surface heat-transfer distributions.

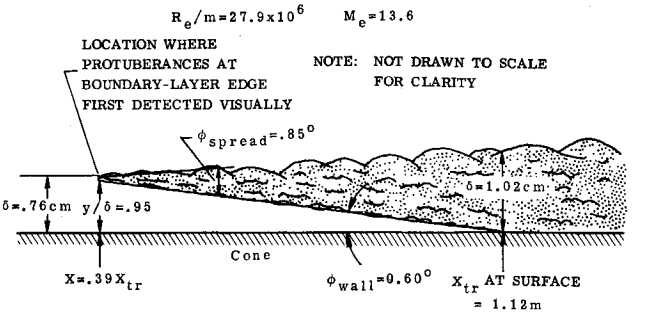

Fig. 3 Growth of turbulence in a hypersonic boundary layer based on schlieren photographs and surface heat transfer.

flows the boundary-layer mean profiles may be highly transitional in the outer part of the boundary-layer before the transition process is detected at the surface, as briefly discussed in earlier studies.[11,12] An examination of boundary-layer mean profiles labeled laminar by previous investigators[4,6] at hypersonic Mach numbers suggests a transitional outer profile as in the present case. The numerical methods which compute the development of boundary-layer profiles and thickness parameters given some upstream initial conditions may experience difficulty with hypersonic flows of this type. Because the transition process initiates in the outer part of the boundary layer, a means of determining and inputting this initial location in the computation method must be devised. As an example, for the low Reynolds number case, appreciable waviness at the boundary-layer edge was perceivable as far upstream as $x = 0.39x_{tr}$ and a disturbance spreading angle can be crudely determined to be $\phi_{spread} = 0.85°$ (0.60° relative to the wall), assuming the disturbance initiates at the critical layer,[13] $y/\delta = 0.95$ as shown in Fig. 3. Hot-wire and hot-film surveys[4,5,7,12] of the "laminar" boundary layer upstream of transition indicated initial disturbances at or near the critical layer. Spreading angles relative to the wall (knowing the wall transition location) were determined by the present authors to be approximately constant ($\phi_{wall} = 0.5°$–$1.0°$) for $M_e = 2.5$–13.6. Since the location of the critical layer moves outward in the boundary layer with increasing Mach number,[13] the relatively constant spreading angle implies a greater "upstream influence" of boundary-layer transition as Mach number increases. The initial protuberance location is believed important since the mean properties of the boundary layer may be affected from this point downstream. In addition, the turbulence terms (eddy viscosity, intermittency, etc.) which govern the disturbance growth from the outer transitional location down to the wall must be properly modeled in order to compute accurate transitional-turbulent flow development, for instance by the methods of Refs. 14 and 15.

References

[1] Moore, F. K., "Theory of Laminar Flows," *High Speed Aerodynamics and Jet Propulsion*, Vol. 4, Princeton University Press, Princeton N. J., 1964.

[2] Schubauer, G. B. and Skramstad, H. K., "Laminar-Boundary-Layer Oscillations and Transition on a Flat Plate," Rept. 909, 1948, NACA.

[3] Schubauer, G. B. and Klebanoff, P. S., "Contributions on the Mechanics of Boundary-Layer Transition," Rept. 1289, 1956, NACA.

[4] Maddalon, D. V. and Henderson, A., Jr., "Boundary-Layer Transition on Sharp Cones at Hypersonic Mach Numbers," *AIAA Journal*, Vol. 6, No. 3, March 1968, pp. 424–431.

[5] Owen, F. K., "Fluctuation and Transition Measurements in Compressible Boundary Layers," AIAA Paper 70-745, Los Angeles, Calif., 1970.

[6] Softley, E. J. and Graber, B. C., "Experimental Observations of Transition of the Hypersonic Boundary Layer," *AIAA Journal*, Vol. 7, No. 2, Feb. 1969, pp. 257–263.

[7] LaGraff, J. E., "Observations of Boundary-Layer Transition in a Mach 7 Gun Tunnel with a Hot-Wire Anemometer," AIAA Paper 71-199, New York, 1971.

[8] Morkovin, M. V., "Critical Evaluation of Transition From Laminar to Turbulent Shear Layers with Emphasis on Hypersonically Traveling Bodies," AFFDL-TR-68-149, March 1969, Air Force Flight Dynamics Lab., Wright-Patterson Air Force Base.

[9] Potter, J. L. and Whitfield, J. P., "Boundary Layer Transition under Hypersonic Conditions," AGARDograph 97, Pt. 3, 1965.

[10] Beckwith, I. E. and Cohen, N. B., "Application of Similar Solutions to Calculation of Laminar Heat Transfer on Bodies with Yaw and Large Pressure Gradient in High-Speed Flow," TN D-625, 1960, NASA.

[11] Henderson, A., Jr., Rogallo, R. S., Woods, W. C., and Spitzer, C. R., "Exploratory Hypersonic Boundary-Layer Transition Studies," *AIAA Journal*, Vol. 3, No. 7, July 1965, pp. 1363–1364.

[12] Staylor, W. F. and Morrisette, E. L., "Use of Moderate-Length Hot Wires to Survey a Hypersonic Boundary Layer," *AIAA Journal*, Vol. 5, No. 9, Sept. 1967, pp. 1698–1700.

[13] Stainback, P. C., "Use of Rouse's Stability Parameter in Determining the Critical Layer Height of a Laminar Boundary Layer," *AIAA Journal*, Vol. 8, No. 1, Jan. 1970, pp. 173–175.

[14] Harris, J. E., "Numerical Solution of the Equations for Compressible Laminar, Transitional, and Turbulent Boundary Layers and Comparisons with Experimental Data," TR R-368, Aug. 1971, NASA.

[15] Adams, J. C., Jr., "Eddy Viscosity-Intermittency Factor Approach to Numerical Calculation of Transitional Heating on Sharp Cones in Hypersonic Flow," AEDC-TR-70-210, Nov. 1970, Arnold Engineering Development Center, Arnold Air Force Station, Tenn.

Cross-Hatching as an Aeroviscoelastic Problem

EARL H. DOWELL*
Princeton University, Princeton, N.J.

PROBSTEIN and Gold[1] have recently given an analysis of the phenomena of "cross-hatching," i.e., the formation of diamond-shaped patterns on the surface of bodies exposed to a supersonic flow. In their theoretical model, the cross-hatching results from the instability of a coupled fluid-(viscoelastic) solid interaction, hence one might term it an "aeroviscoelastic" problem. Whatever one calls it, the considerable experience developed in the field of aeroelasticity may be used to gain further insight into their model and its possible relevance to cross-hatching. In particular, we shall use the methods and to some extent the results of Ref. 2 and references cited therein to assess the Probstein-Gold model.

Analysis of Probstein-Gold Model

An inviscid, potential flow model is employed where the perturbation pressure p' satisfies (the notation is that of Ref. 1)

$$(1-M^2)\partial^2 p'/\partial x^2+\partial^2 p'/\partial y^2=(M^2/U^2)(\partial/\partial t)(\partial p'/\partial t+2U\,\partial p'/\partial x) \tag{1}$$

The boundary condition at the fluid-solid interface is

$$\rho(D^2\delta/Dt^2)=-\partial p'/\partial y|_{y=0} \tag{2}$$

where δ is the vertical solid displacement. The equation of motion of the viscoelastic solid is taken to be

$$\tau(D/Dt)\partial\delta/\partial x=\kappa p'-\partial\delta/\partial x \tag{3}$$

We examine traveling wave solutions which assumes the finite dimensions of the solid are, in some sense, unimportant.

Assume

$$\delta=\bar{\delta}\,e^{i\omega t+i\alpha x};\quad p'=\bar{p}\,e^{i\omega t+i\alpha x}$$

From Eq. (1)

$$(i\alpha)^2[1-M^2(1+i\omega/Ui\alpha)^2]\bar{p}+d^2\bar{p}/dy^2=0$$

The two independent solutions are

$$\bar{p}=e^{\pm i\alpha[M^2(1+i\omega/Ui\alpha)^2-1]^{1/2}y} \tag{4}$$

We shall select the minus sign to satisfy the Sommerfeld condition. (This point is actually more subtle, see Ref. 2 and references cited therein.) From Eq. (2)

$$\rho(i\omega+Ui\alpha)^2\bar{\delta}=-\partial\bar{p}/\partial y|_0$$

From Eq. (3)

$$i\alpha[\tau(i\omega+Ui\alpha)+1]\bar{\delta}=\kappa\bar{p}$$

Combining the above two equations

$$\rho(i\omega+Ui\alpha)^2\kappa\bar{p}/i\alpha[\tau(i\omega+Ui\alpha)+1]=-\partial\bar{p}/\partial y|_{y=0} \tag{5}$$

Using Eq. (4) in Eq. (5) and cancelling out common factors

$$\rho(i\omega+Ui\alpha)^2\kappa/i\alpha[\tau(i\omega+Ui\alpha)+1]=i\alpha[M^2(1+i\omega/Ui\alpha)^2-1]^{1/2} \tag{6}$$

This is the eigenvalue equation to determine the permissible values of ω. Equation (6) is not given explicitly in Ref. 1, but presumably was obtained by Probstein-Gold.

At this point the authors of Ref. 1 assumed the instability was a static one (presumably based upon experimental observations) and assumed consequently that ω was a purely imaginary number. They then sought solutions of maximum growth rate as a function of the problem parameters from Eq. (6) or their equivalent of same. We shall return to their approach later but for the moment shall pursue a different approach.

Introduce nondimensional variables and parameters as follows:

$$\Omega\equiv i\omega/Ui\alpha,\quad \tau U\alpha\equiv\varepsilon^*,\quad \rho U^2\kappa\equiv\lambda^*$$

From Eq. (6)

$$\lambda^*[\Omega+1]^2/[i\varepsilon^*(\Omega+1)+1]=[M^2(1+\Omega)^2-1]^{1/2} \tag{7}$$

Hence, we see that

$$\Omega=\Omega(\lambda^*,M,\varepsilon^*)$$

Further define

$$\lambda\equiv\lambda^*/M^2$$
$$X\equiv M(1+\Omega)$$
$$\varepsilon\equiv\varepsilon^*/M$$

then Eq. (7) may be written even more compactly

$$E\equiv\lambda X^2/[i\varepsilon X+1]=(X^2-1)^{1/2}\equiv F \tag{8}$$

and hence, $X=X(\lambda,\varepsilon)$.

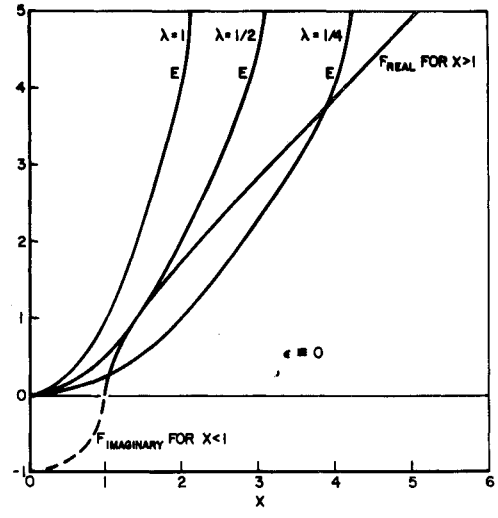

Fig. 1 Graphical solution to eigenvalue equation.

Received September 30, 1971; revision received December 17, 1971. The author would like to thank the reviewer for a number of helpful comments.

Index categories: Supersonic and Hypersonic Flow; Aeroelasticity and Hydroelasticity.

* Department of Aerospace and Mechanical Sciences. Member AIAA.